



Fracture criteria identification using an inverse technique method and blanking experiment

Ridha Hambli^{a,*}, Marian Reszka^b

^a*ISTIA - LASQUO, 62, Avenue Notre Dame du Lac, 49000 Angers, France*

^b*ENSAM - LPMI, - 2, Bld du Ronceray, - B.P 3525, 49035 Angers cedex, France*

Received 28 February 2001; received in revised form 8 April 2002

Abstract

In order to optimize the blanking processes, it is important to identify the conditions within the deforming workpiece which may lead to fracture initiation and propagation. Within this framework, numerical simulations are widely used in industries to optimize sheet metal forming processes. However, in order to have a confidence in the results of such simulations, an accurate material model is required. The accuracy of a material model is affected by the constitutive equations and the values of the material parameters. In order to reduce the danger of fracture of metal parts during manufacturing processes, advanced optimal design requires knowledge of critical values of some fracture criteria of the material used. Experimental identification of fracture criteria are currently obtained by performing several complicated tests and long duration of experiments.

This study presents a computation methodology allowing for the identification of critical values of fracture criteria in order to simulate crack initiation and propagation generated by shearing mechanisms, which are needed for metal blanking processes simulation. The approach is based on inverse technique using circular blanking experiments and finite element calibration model. The critical values of fracture criteria are obtained in such a way that the finite element force–penetration predicted curve fit the experimental plot deduced from blanking tests. The numerical results obtained by the simulation were compared with experimental ones to verify the validity of the proposed technique for fracture criteria identification.

© 2002 Elsevier Science Ltd. All rights reserved.

Keywords: Fracture criteria; Inverse technique; Blanking; Finite element; Experiment

1. Introduction

To be successful in today's world market, Products must be designed with parameters that ensure high levels of reliability and quality. Generally, new products contain many quality and reliability

* Corresponding author. Tel.: +33-2-4136-5757; fax: +33-2-4136-5743.

E-mail address: ridha.hambli@istia.univ-angers.fr (R. Hambli).

problems [1–3]. The optimal design of the manufacturing processes can certainly improve the quality of the parts.

Nowadays, computer simulation of metal parts gives important contribution for the understanding and prediction of sheet metal behavior. In general, the process involves large deformation of the material and many physical phenomena, such as damaging, may occur [4,5]. The damage which results in a progressive degradation of the metal can lead to the failure of the parts during the forming processes [1,6–8]. The experience shows that it is possible to avoid or to reduce failure modes within the products by the optimal designing of the forming processes [2,3].

In sheet metal forming processes, the first step involves cutting of the sheet into appropriate shapes by means of the physical process of shearing. A contoured part is cut between a punch and die in a press. Depending on the position of the sheared surface with respect to the workpiece coordinates, various shearing processes are used, such as punching, blanking, piercing and cutting off. Contrary to other operations, such as stamping and bending where the aim is to plastically deform the sheet, these operations lead to the total rupture of the sheet. Before complete rupture, the material is subjected to some phenomena of damage and crack propagation. To describe the sheet's behavior as the operation is carried out, various parameters may be used such as the material hardening, the damage evolution and the cracks initiation and propagation.

One major difficulty in the numerical analysis of blanking processes is the accurate description of ductile fracture initiation, which greatly determines the product shape [3,5,9].

The present investigation is focussed on the computation methodology of critical values of fracture criteria in order to simulate crack initiation and propagation generated by shearing mechanisms like blanking processes.

The approach is based on an inverse technique using circular blanking experiments and finite element calibration.

2. Numerical modelling of ductile fracture

In blanking processes, when the critical values of some fracture criteria are known for a given material, it should be possible to predict the crack initiation and propagation within the sheet. The fracture of ductile material has frequently been observed to result from the large growth and coalescence of microscopic voids, a mechanism enhanced by the superposition of hydrostatic stress on a plastic deformation field [10–12]. The damage phenomenon, described by initiation and growth of cavities and microcracks into the material induced by large deformations in metals, has been extensively studied in order to predict the ductile damage evolution into structures subjected to plastic loading [10,12]. In order to predict when a structure will undergo rupture, numerous authors have proposed their own criteria [6–8,10]. Fracture initiates when the integrated product of the equivalent plastic strain increment and a function depending on some material parameters and stresses and/or strains components exceeds a critical value. Most of the published fracture criteria are based on the concentration of plastic strain. This macroscopic variable appears to capture the essential physics of microscopic fracture process. While based on plastic strain, some fracture criteria also include the effect of hydrostatic tensile stress. It is well known that ductility increases when hydrostatic tension decreases [9,12].

The failure is modelled by a mathematical function which is assumed to represent the physical behavior of the material, and occurs when the function reaches a critical value C_c .

Table 1
Fracture criteria

Fracture criteria	Function	
Rice and Tracey [12]	$\int_0^{\varepsilon_R} \exp\left(1.5 \frac{\sigma_H}{\sigma_{eq}}\right) d\varepsilon_{eq} - C1 = 0$	σ_{eq} is the Von Mises stress, σ_H the hydrostatic pressure
Freudenthal (1950) [2,4]	$\int_0^{\varepsilon_R} \sigma_{eq} d\varepsilon_{eq} - C2 = 0$	
Cockcroft and Latham [6]	$\int_0^{\varepsilon_R} \frac{\Omega}{\sigma_{eq}} d\varepsilon_{eq} - C3 = 0$	
Brozzo (1972) [2,4]	$\int_0^{\varepsilon_R} \frac{2}{3} \left(\frac{\Omega}{\Omega - \sigma_H} \right) d\varepsilon_{eq} - C4 = 0$	$\Omega = \text{Max}(\sigma_1, \sigma_2, \sigma_3, 0)$ where $\sigma_1, \sigma_2, \sigma_3$ are the principal stresses
Ghosh (1976) [2,4]	$\left(\frac{\sigma_I - \sigma_{III}}{2} \right) \sigma_H - C5 = 0$	
Norris (1978) [2,4]	$\int_0^{\varepsilon_R} \left(\frac{1}{1 - c\sigma_H} \right) d\varepsilon_{eq} - C6 = 0$	$c = 0.7 \text{ GPa}^{-1}$: material constant
Atkins [21,22]	$\int_0^{\varepsilon_R} \left(\frac{1 + 1/2L}{1 - c\sigma_H} \right) d\varepsilon_{eq} - C7 = 0$	c is a material constant and $L = d\varepsilon_1/d\varepsilon_2$
Oyane (1980) [2,4]	$\int_0^{\varepsilon_R} \left(1 + A \frac{\sigma_H}{\sigma_{eq}} \right) d\varepsilon_{eq} - C8 = 0$	$A = 0.424$: material constant
Ayada	$\int_0^{\varepsilon_R} \left(\frac{\sigma_H}{\sigma_{eq}} \right) d\varepsilon_{eq} - C9 = 0$	
Plastic strain	$\varepsilon_{eq} - C10 = 0$	Equivalent plastic strain

The fracture functions are often written in the following form:

$$\text{if } \int_0^{\varepsilon_R} f(\sigma, \varepsilon_{eq}) d\varepsilon_{eq} - C_c < 0 \text{ there is no failure,} \quad (1)$$

$$\text{if } \int_0^{\varepsilon_R} f(\sigma, \varepsilon_{eq}) d\varepsilon_{eq} - C_c \geq 0 \text{ the failure occurs.} \quad (2)$$

In the above expressions, ε_R is the strain at rupture, ε_{eq} is the equivalent plastic strain defined by means of the plastic part

$$\varepsilon_{eq} = \sqrt{\frac{2}{3} \varepsilon_{ij}^{pl} \varepsilon_{ij}^{pl}}. \quad (3)$$

Different failure criteria of structures subjected to external elastoplastic forces have been detailed by Hambli [5] (Table 1).

There exists a wide variety of criteria for assessing rupture in metal forming processes [2,4,5].

However, the calibration of fracture criteria is an important stage in order to obtain reliable results for blanking simulation [10,13].

Much works has shown that it is difficult to chose a fracture criteria that is “universal” enough in the sense that it gives consistent results also for operating conditions outside the calibration range [2,4,14–17]. Application of critical values of fracture criteria are only successful when they are both characterized and applied under similar loading conditions.

3. Finite element approach

Experiments using devices equipped with electrical gauges and force transducer were performed using 4000 kN hydraulic press (Fig. 1) for the identification of some fracture criteria.

The problem studied here consists of an axisymmetric blanking operation (Fig. 2) of a sheet-metal with 3.5 mm thickness.

The constitutive equations describing the material behavior should allow for the description of the different stages of the deformation including fracture initiation and propagation phenomena. For this purpose, a behavioral law coupled with failure criteria must be chosen.

In the case of blanking process, in the shearing zone, the stress condition during crack formation is triaxial (Fig. 3). According to Tresca, the flow criterion is

$$\tau_{\max} = \frac{\sigma_1 - \sigma_3}{2}, \quad (4)$$



Fig. 1. Experimental setup of blanking experiment.

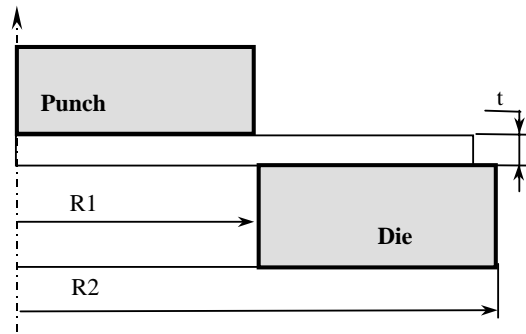


Fig. 2. Axisymmetric model of the blanking operation.

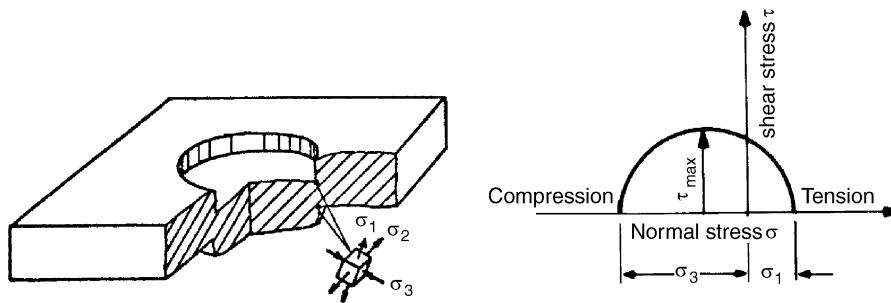


Fig. 3. Stress conditions in shearing from Ref. [3].

where σ_1 , σ_2 and σ_3 are the principal tensile stress, the tangential tensile stress and the principal compressive stress.

The stress condition changes throughout the deformation process. At the initiation of the cracks, τ_{\max} reaches the fracture limit before the yielding limit. The cracks are propagated in the direction of maximum shear stress.

Fracture criteria models has been implemented in the implicit finite element code ABAQUS/Standard [18] as well as an optimization algorithm based on sensitive optimization methods. This technique is frequently used in topology and shape optimization analysis.

The algorithms generally implemented in the finite element codes for integration of non-linear constitutive equations are the so-called radial return algorithms, and they are used to solve the equations in an incremental form. They are based upon the notion of an elastic predictor–plastic corrector where a purely elastic trial state is followed by a plastic corrector phase [18–20]. In this way, an implicit algorithm has been developed which allows for the integration of the constitutive equations. The computational scheme which seems to be well adapted to the non-linearity of the behavioral law [18–20] is briefly summarized in the following. The integration methods of the non-linear constitutive equations are based on the use of a special algorithm which solves the equations in incremental form. For this purpose, during a small time interval $[t_n, t_{n+1}]$, it is assumed that the whole increment is purely elastic, then an elastic prediction is defined as

$$\sigma_{n+1}^T = \sigma_n + \Delta\sigma. \quad (5)$$

Then Eq. (5) can be written as

$$\sigma_{n+1}^T = \mathbf{C}_{el}(\varepsilon_{n+1} - \varepsilon_n^{pl}). \quad (6)$$

Superscript T refers to Trial test and \mathbf{C}_{el} is the elastic modulus tensor.

ε_{n+1} is the total strain tensor at increment $n + 1$ and ε_n^{pl} is the plastic part of the strain tensor at increment n .

The von Mises yield function is given by

$$f = \sigma_{eq} - (\sigma_{el} + \sigma_0), \quad (7)$$

where σ_{el} is the initial yield stress obtained by a tensile test and σ_0 is the non-linear strain hardening law.

If this elastic prediction satisfies the yield condition: $f < 0$, the prediction is true and the local procedure is completed. Then it can be stated that

$$\sigma_{n+1} = \sigma_{n+1}^T. \quad (8)$$

Otherwise, this state must be corrected by means of a plastic correction. The variables at increment $n + 1$ must satisfy the yield condition, i.e. the evolution laws written in the incremental form and elasticity law must satisfy the system

$$f = 0, \quad (9)$$

$$\sigma_{n+1} - \mathbf{C}_{el}(\varepsilon_n + \Delta\varepsilon - \varepsilon_n^{pl} - \Delta\varepsilon^{pl}) = 0, \quad (10)$$

$$\Delta H^\alpha = h^\alpha(\Delta\varepsilon_{ij}, (\sigma_{ij})_{n+1}, H_{ij}^\alpha), \quad (11)$$

where H^α , $\alpha = 1, 2, \dots, n$, is a set of scalar state variables and h^α is the hardening law for H^α .

Within the framework of the displacement formulation of FEM, the global equilibrium equations to be satisfied at each instant t_{n+1} can be written in the general form [18]

$$\mathbf{F}(\mathbf{U}_{n+1}) = 0, \quad (12)$$

where \mathbf{U}_{n+1} is the displacement field at step $(n + 1)$.

If this non-linear problem is solved iteratively by a Newton method, at each global iteration r the following equation can be written:

$$\mathbf{F}(\mathbf{U}_{n+1}^r) + (\mathbf{K}_{n+1}^r)(\mathbf{U}_{n+1}^{r+1} - \mathbf{U}_{n+1}^r) = 0, \quad (13)$$

where

$$\mathbf{K}_{n+1}^r = \left(\frac{\partial \mathbf{F}}{\partial \mathbf{U}} \right)_{n+1}^r = \int_{\Omega} \mathbf{B}^T \mathbf{J}_{n+1}^r \mathbf{B} d\Omega, \quad (14)$$

where \mathbf{B} is the strain–displacement matrix and \mathbf{J}_{n+1}^r is the Jacobian tensor obtained by

$$\mathbf{J}_{n+1}^r = \left(\frac{\partial \boldsymbol{\sigma}}{\partial \boldsymbol{\varepsilon}} \right)_{n+1}^r. \quad (15)$$

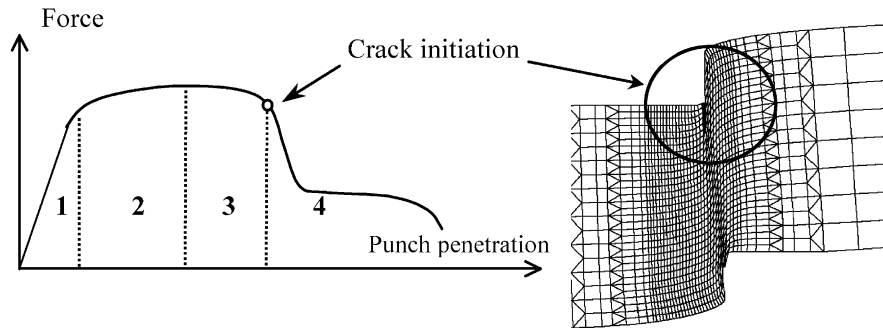


Fig. 4. Schematic diagram of blanking force vs. punch penetration after Ref. [5]. 1—Elastic stage. 2—Elastoplastic stage. 3—Elastoplastic stage in which damage occurs. 4—Initiation and propagation of cracks leading to final rupture.

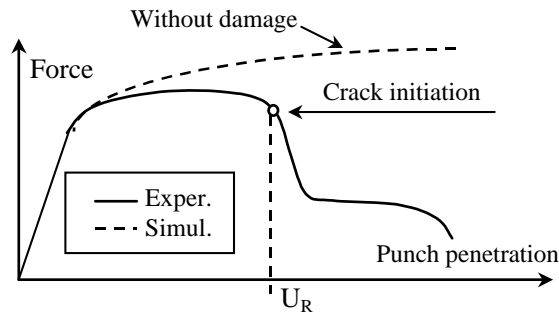


Fig. 5. Illustration of the difference between the predicted and the experimental force–penetration curves.

4. Prediction of the critical fracture criteria

Different investigations [5,21,22] have shown that during blanking process, the sheet-metal fracture affects the blanking force–penetration curve illustrated in Fig. 4.

The prediction method developed in this work, gives the fracture criteria critical value of the material. The approach consists in minimizing the difference between the punch penetration prior to rupture values (U_R) obtained by the blanking experiment and deduced from the finite element simulation. From a numerical point of view, the computational algorithm is based on an iterative scheme. The aim is to minimize an objective function in order to reduce the difference between the computed and the experimental values of penetration U_R (Fig. 5).

During the optimization process a multi-variable objective function Φ was chosen in the following form:

$$\Phi = \frac{U_R^e - U_R^s}{U_R^e}, \quad (16)$$

where U_R^e and U_R^s are experimental and numerical punch penetration at rupture.

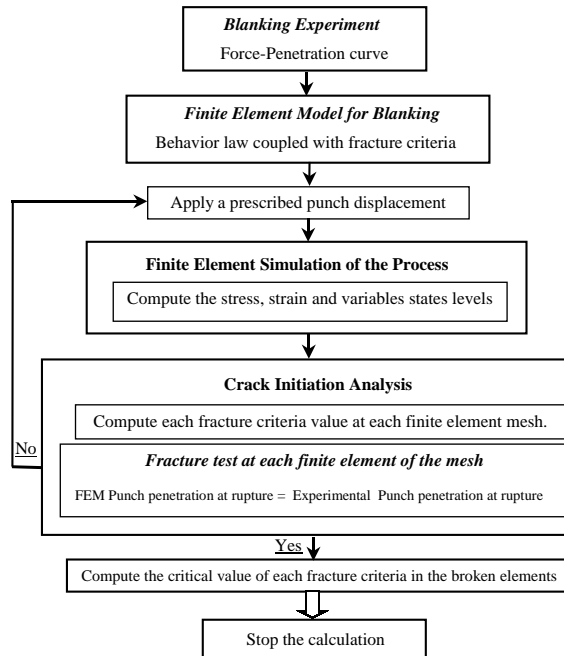


Fig. 6. Flow chart of the calibration method.

The criteria of convergence is such that the numerical results must satisfy the condition

$$\Phi \leq Tol., \quad (17)$$

where *Tol.* is tolerance values for convergence given by the user.

The optimal values of material model parameters can be obtained by performing a series of numerical analyses in order to pursue a minimum function error Φ .

The iterative finite element program including the algorithm of the fracture criteria characterization is schematically represented by the flow chart of Fig. 6.

The described procedure has been implemented in the finite element code ABAQUS/Standard with the help of the user subroutine UMAT [18].

5. Results and discussion

The mechanical characteristics of the material obtained by a tensile test are

$$E = 210000 \text{ MPa}, \quad \nu = 0.29.$$

The corresponding strain hardening law takes the non-linear form

$$\sigma = \sigma_{el} + K \varepsilon_{pl}^n \quad (18)$$

with the values of $\sigma_{el} = 250 \text{ MPa}$, $K = 1048 \text{ MPa}$, $n = 0.196$.

The meshing of the model is carried out by means of 1400 quadrangular four-node axisymmetric elements. Fig. 7 shows how the mesh has been constructed.

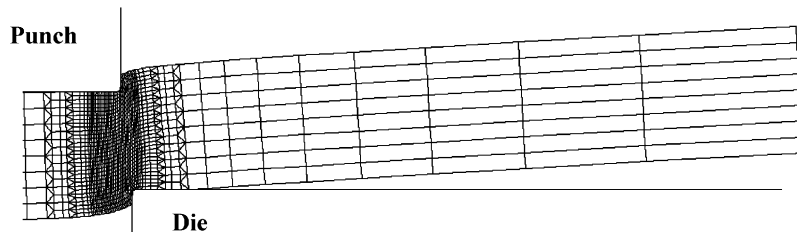


Fig. 7. Mesh used for the FE model.

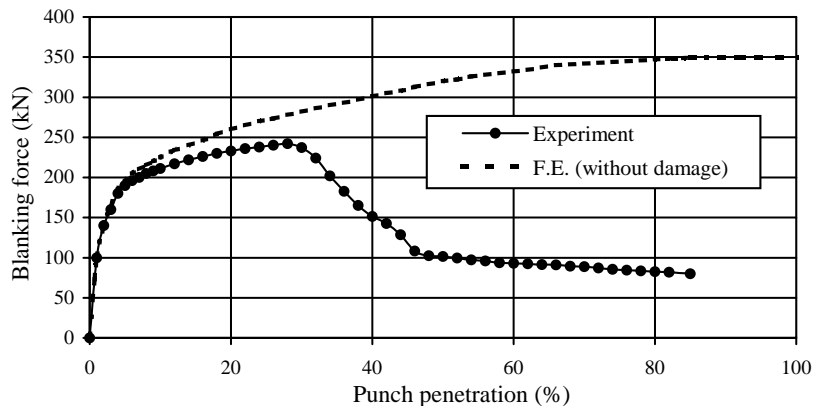


Fig. 8. Blanking force–penetration curve evolution.

In a simplified modelling, the blanking process was performed neglecting damage evolution leading to crack initiation and propagation into the sheet. Using the aforementioned elastoplastic constitutive laws, it is possible to simulate the punch penetration up to 100% of the sheet's thickness, in spite of a large mesh distortion.

The force–penetration curves obtained by experiment and numerical calculation are plotted in Fig. 8.

It can be noted that there is a difference between both curves. This difference is due to the fact that during the simulation, the damage evolution was not accounted for. Consequently, the predicted curve evolution exceeds the experimental one. It can be concluded that to be accurately predicted, the blanking process would necessarily account for fracture initiation and propagation.

The experimental curve shows that cracks initiate within the specimen for a punch penetration of about 32% of the sheet thickness. Therefore, the critical value of the fracture criteria can be computed at this deformed configuration. When the fracture threshold is satisfied within an element, the element fractures and cracks occur. The direction of crack propagation and the crack tip position are then determined by the value contour of the fracture criteria value at each element of the mesh.

For the simulation of processes where rupture is to be considered, it is necessary to develop and apply methods using mechanical fracture models where a material separation must be predicted. There are at least four possible methods to simulate a crack propagation in a finite element mesh,

Table 2

Critical values of the fracture criteria predicted by the simulation

Fracture criteria	Function	Critical value	Validity of the criteria
Rice and Tracey	$\int_0^{\varepsilon_R} \exp\left(1.5 \frac{\sigma_H}{\sigma_{eq}}\right) d\varepsilon_{eq} - C1 = 0$	$C1 = 1.6$	Good
Freudenthal	$\int_0^{\varepsilon_R} \sigma_{eq} d\varepsilon_{eq} - C2 = 0$	$C2 = 4260$	Good
Cockroft and Latham	$\int_0^{\varepsilon_R} \frac{\Omega}{\sigma_{eq}} d\varepsilon_{eq} - C3 = 0$	$C3 = 0.455$	Good
Brozzo	$\int_0^{\varepsilon_R} \frac{2}{3} \left(\frac{\Omega}{\Omega - \sigma_H} \right) d\varepsilon_{eq} - C4 = 0$	$C4 = 1.85$	Bad
Ghosh	$\left(\frac{\sigma_I - \sigma_{III}}{2} \right) \sigma_H - C5 = 0$	$C5 = 3.25$	Bad
Norris	$\int_0^{\varepsilon_R} \left(\frac{1}{1 - c\sigma_H} \right) d\varepsilon_{eq} - C6 = 0$	$C6 = 1.165$	Bad
Atkins	$\int_0^{\varepsilon_R} \left(\frac{1 + 1/2L}{1 - c\sigma_H} \right) d\varepsilon_{eq} - C7 = 0$	$C7 = 1.72$	Good
Oyane	$\int_0^{\varepsilon_R} \left(1 + A \frac{\sigma_H}{\sigma_{eq}} \right) d\varepsilon_{eq} - C8 = 0$	$C8 = 2.455$	Good
Ayada	$\int_0^{\varepsilon_R} \left(\frac{\sigma_H}{\sigma_{eq}} \right) d\varepsilon_{eq} - C9 = 0$	$C9 = 0.52$	Good
Plastic strain	$\varepsilon_{eq} - C10 = 0$	$C10 = 4.2$	Good

including element splitting, separating of nodes, element deletion and stiffness FE decreasing. This last technique has been retained in this work in order to simulate crack propagation. During the analysis, the initiation of crack is assumed to occur at any point in the mesh where the fracture criteria reaches its critical value C_c . The crack propagation is simulated by the propagation of a completely damaged area. From a numerical point of view, this method leads to the decrease in the stiffness of the damaged finite elements.

Applying the algorithm of the flow chart in Fig. 6, the critical values of the fracture criteria predicted by the proposed identification technique are reported in Table 2. Different blanking simulations has been performed using the different fracture criteria of Table 2. The validity of each criteria is commented in the last column of the table. The best criterion seems to be the Rice and Tracey one which take into account the influence of the hydrostatic pressure.

The quality of the blanked parts are connected to the geometry of the sheared edge such as the roll-over depth, the fracture depth, the smooth-sheared depth, the burr formation and the fracture angle (Fig. 9).

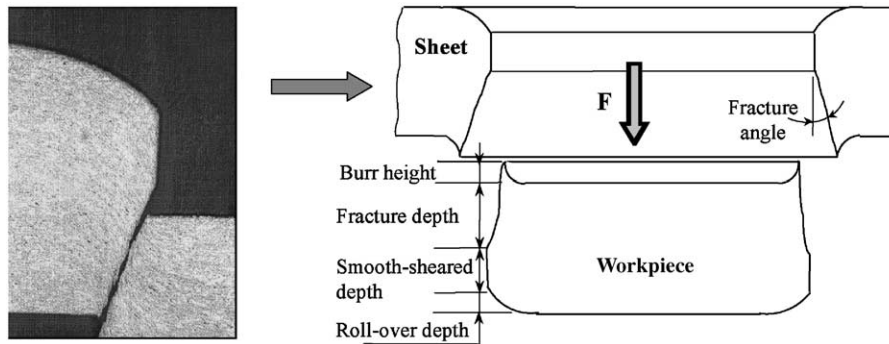
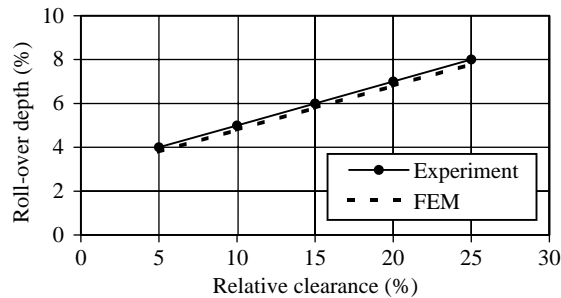


Fig. 9. Geometry of the sheared workpiece.

Fig. 10. Evolution of the roll-over depth (H_{bb}) vs. the clearance.

In order to check the fracture criteria validity in blanking modelling, different FEM simulations have been performed for different clearances.

Fig. 10 illustrates the evolution of the roll-over depth H_{bb} vs. the clearance obtained by experiments of blanking on 1060 steel sheet and numerically.

It can be shown that H_{bb} depth evolves linearly according to the clearance.

The evolution of the sheared zone depth H_l vs. the clearance obtained by numerical calculation is compared with the experimental results (Fig. 11).

It can be observed, that the predicted and experimental curves coincide very well even for high and small clearances. The results shows the strong dependence between the sheared area depth and clearances in the range 2–10%. For clearances greater than 10%, H_l depth variation is uniform.

The punch penetration corresponding to crack initiation vs. clearance from both numerical calculation and experiments are plotted in Fig. 12.

The experimental curve shows that the smallest penetration causing the rupture of sheet is that which corresponds to the clearance $c = 15\%$. It can be shown that results are in good agreement.

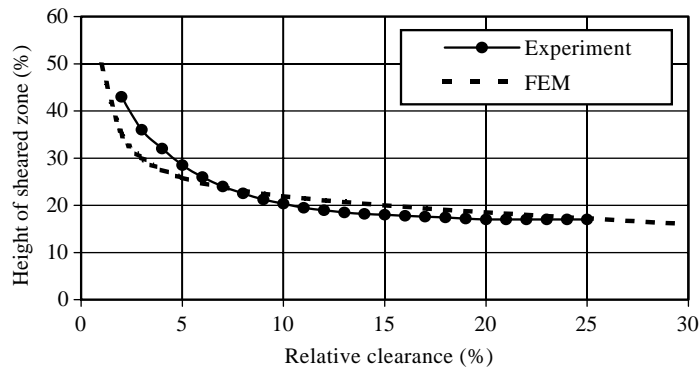


Fig. 11. Evolution of the sheared zone depth (H_I) vs. the clearance.

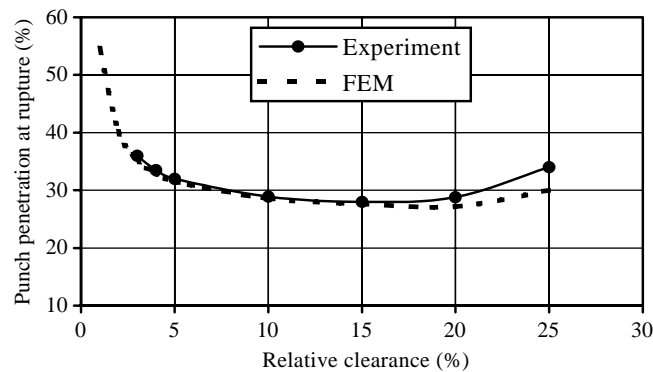


Fig. 12. Punch penetration corresponding to the crack initiation vs. clearance.

6. Conclusion

This paper has described an inverse technique approach using the FEM. The model allows for the identification of the critical values of fracture criteria valid for crack initiation modelling generated by shearing mechanisms. The proposed identification technique is based on a simulation-experiment coupled approach using blanking experiments. The aim is to minimize an objective function in order to reduce the difference between the computed and the experimental values of the blanking force–penetration curve. The critical values of the fracture criteria are then calibrated by computer-simulated blanking experiments of circular process.

The proposed methodology can be used for blanking processes design to choose the process leading parameters in an optimal way that ensure a high-quality part.

Acknowledgements

The authors thank Professors Alain Potiron and Daniel Badie-Levet for their assistance during this investigation and Deville S.A. Company for its support.

References

- [1] Hambli R, Badie-Levet D. Damage and fracture simulation during the extrusion processes. *Computer Methods in Applied Mechanics and Engineering* 2000;186:109–20.
- [2] Hartley P, Pillinger I, Sturgess CEN. Numerical modeling of material meformation processes research, development and applications. Berlin: Springer, 1992.
- [3] Kurt L. Handbook of metal forming. New York: McGraw-Hill, 1985.
- [4] Clift SE, Hartley P, Sturgess CEN, Rowe GW. Fracture prediction in plastic deformation process. *International Journal of Mechanical Sciences* 1990;32(1):1–17.
- [5] Hambli R. Etude expérimentale, numérique et théorique du découpage des tôles en vue de l'optimisation du procédé. Thesis dissertation, ENSAM d'Angers, 1996 [In French].
- [6] Cockroft MG, Latham DJ. A simple criterion for fracture for ductile-fracture of metals. National Engineering Laboratory, Report No. 240, 1966.
- [7] Morris DM, Reaugh JE, Morgan B, Quinones DF. A plastic-strain, mean stress criterion for ductile fracture. *Journal of Engineering Materials and Technology* 1978;100(3):279–86.
- [8] Oyane M, Sato T, Okimoto K, Shima S. Criteria for ductile fracture and their application. *Journal of Mechanical Working Technology* 1980;4:65–81.
- [9] Hambli R. Finite element simulation of fine blanking processes using a pressure-dependant damage model. *Journal of Materials Processing Technology* 2001;116(2–3):252–64.
- [10] McClintock FA. A criterion for ductile fracture by the growth of holes. *Journal of Applied Mechanics* 1968;35:363–71.
- [11] McClintock FA, Kaplan SM, Berg A. Ductile fracture by hole growth in shear bands. *International Journal of Fracture Mechanics* 1966;2:614–27.
- [12] Rice JR, Tracey DM. On the ductile enlargement of voids on triaxial stress fields. *Journal of Mechanics and Physics of Solids* 1969;17:201–17.
- [13] Fischer FD, Kolednik O, Shan GX, Rammerstorfer FG. A note on calibration of ductile failure damage indicators. *International Journal of Fracture* 1995;73:345–57.
- [14] Atkins AG. Fracture mechanics and metalforming: damage mechanics and the local approach of yesterday and today. In: Rossmann HP, editor. *Fracture research in retrospect*. Rotterdam: Balkema, 1997. p. 327–50.
- [15] Wifi AS, El-Abbasi N, Abdel-Hamid A. A study of workability criteria in bulk forming processes. In: Ghosh SK, Predeleanu M, editors. *Materials processing defects*. Amsterdam: Elsevier, 1995. p. 333–57.
- [16] Zhu YY, Cescotto S, Habraken AM. Modelling of fracture initiation in metalforming processes. In: Ghosh SK, Predeleanu M, editors. *Materials processing defects*. Amsterdam: Elsevier, 1995. p. 155–79.
- [17] Gouveia BPPA, Rodrigues JMC, Martins PAF. Fracture predicting in bulk metal forming. *International Journal of Mechanical Sciences* 1996;38:361–72.
- [18] ABAQUS. Theory manual. Version 6.2.
- [19] Criesfield MA. Non linear finite element analysis of solids and structures, vol. 1. New York: Wiley, 1991.
- [20] Marques JMMC. Stress computation in elastoplasticity. *Engineering and Computers* 1984;1:42–51.
- [21] Atkins AG. Surfaces produced by guillotining. *Philosophical Magazine* 1981;43(3):627–41.
- [22] Atkins AG. Possible explanation for unexpected departures in hydrostatic tension–fracture strain relations. *Metal Science* 1981;81:81–3.